J. Am. Soc. Mass Spectrom. (2015) 26:774–781
DOI: 10.1007/s13361-015-1080-7

RESEARCH ARTICLE

Formation of a_1 Ions Directly from Oxazolone b_2 Ions: an Energy-Resolved and Computational Study

Benjamin J. Bythell,[1] Alex G. Harrison[2]

[1]Department of Chemistry and Biochemistry, University of Missouri-St. Louis, St. Louis, MO 63131, USA
[2]Department of Chemistry, University of Toronto, Toronto, ON M5S 3H6, Canada

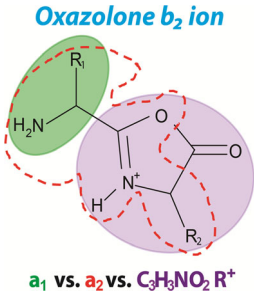

Abstract. It is well-known that oxazolone b_2 ions fragment extensively by elimination of CO to form a_2 ions, which often fragment further to form a_1 ions. Less well-known is that some oxazolone b_2 ions may fragment directly to form a_1 ions. The present study uses energy-resolved collision-induced dissociation experiments to explore the occurrence of the direct $b_2 \rightarrow a_1$ fragmentation reaction. The experimental results show that the direct $b_2 \rightarrow a_1$ reaction is generally observed when Gly is the C-terminal residue of the oxazolone. When the C-terminal residue is more complex, it is able to provide increased stability of the a_2 product in the $b_2 \rightarrow a_2$ fragmentation pathway. Our computational studies of the relative critical reaction energies for the $b_2 \rightarrow a_2$ reaction compared with those for the $b_2 \rightarrow a_1$ reaction provide support that the critical reaction energies are similar for the two pathways when the C-terminal residue of the oxazolone is Gly. By contrast, when the nitrogen of the oxazolone ring in the b_2 ion does not bear a hydrogen, as in the Ala-Sar and Tyr-Sar (Sar=*N*-methylglycine) oxazolone b_2 ions, a_1 ions are not formed but rather neutral imine elimination from the N-terminus of the b_2 ion becomes a dominant fragmentation reaction. The M06-2X/6-31+G(d,p) density functional theory calculations are in general agreement with the experimental data for both types of reaction. In contrast, the B3LYP/6-31+G(d,p) model systematically underestimates the barriers of these S_N2-like $b_2 \rightarrow a_1$ reaction. The difference between the two methods of barrier calculation are highly significant ($P<0.001$) for the $b_2 \rightarrow a_1$ reaction, but only marginally significant ($P=0.05$) for the $b_2 \rightarrow a_2$ reaction. The computations provide further evidence of the limitations of the B3LYP functional when describing S_N2-like reactions.

Keywords: Mass spectrometry, MS/MS, Gas-phase ion structure, b_2 Oxazolone fragmentation, Density functional theory

Received: 19 November 2014/Revised: 13 January 2015/Accepted: 13 January 2015/Published Online: 26 March 2015

Introduction

The fragmentation of protonated peptides, which have been activated by collision, frequently occurs by cleavage at the amide bonds of the peptides [1]. If the charge remains on the N-terminus fragment one obtains a b_n ion while charge retention on the C-terminal fragment leads to a y_n ion [2, 3]. Usually it is these series of b_n and y_n ions resulting from cleavage of the various amide bonds that provide the most significant information as to the amino acid sequence of the peptide. Because of their importance in peptide sequencing, there has been considerable activity in exploring the factors that influence the cleavage reactions occurring as well as the structures and further fragmentation reactions of the primary fragment ions formed.

It has been established [4, 5] that y_n ions are protonated amino acids (y_1) or protonated truncated peptides (y_n) although the prediction as to which y_n ions will be observed still is not straightforward. Initially it was proposed [2, 3] that b_n ions were substituted acylium ions but it has been shown [6–9] that simple b_1 ions (α-aminoacylium ions) are unstable and lose CO exothermically to form the appropriate iminium ion; thus, b_1 ions are rarely observed. On the other hand, larger b_n ($n \geq 2$) ions are regularly observed, suggesting that they do not have an acylium ion structure. Extensive tandem MS studies, H/D exchange studies, and theoretical studies, primarily of simple smaller b_n ions, have provided strong evidence [10–20] for a

Electronic supplementary material The online version of this article (doi:10.1007/s13361-015-1080-7) contains supplementary material, which is available to authorized users.

Correspondence to: Benjamin Bythell; *e-mail:* bythellb@umsl.edu, Alex Harrison; *e-mail:* aharriso@chem.utoronto.ca

protonated oxazolone structure formed by nucleophilic attack by the next adjacent carbonyl group as the amide bond is breaking. The proposed oxazolone structure has been supported by a number of infrared multiphoton dissociation (IRMPD) studies [21–25] of small b_n ions.

An alternative cyclization reaction for b_2 ions involves nucleophilic attack of the N-terminal amine group on the carbonyl function as the amide bond is breaking. This results in formation of a protonated diketopiperazine (cyclic dipeptide). Paizs and Suhai [1] have pointed out that such a cyclization involves a trans-cis isomerization of the first amide bond that is not being broken and that such an isomerization has a significant energy barrier. However, there are a number of cases [26–30] where diketopiperazine formation has been observed. These involve systems where a side-chain group, such as in His and Arg, acts as a catalyst for the isomerization.

The present paper is concerned with the fragmentation reactions of b_2 ions with an oxazolone structure. It is well-known [10, 15, 31] that a major fragmentation channel of oxazolone b_2 ions is elimination of CO to form the a_2 ion. A detailed pathway for this fragmentation reaction has been established from density functional theory and threshold collision-induced dissociation studies [31–33]. It is well-known [32–34] that a_2 ions fragment, in part, to form the a_1 iminium ion. However, it is less well-known that a_1 ions may arise, in some cases, directly by fragmentation of b_2 ions [10, 15, 35]. Again, the detailed pathway has been established from density functional theory and threshold collision-induced dissociation studies [31–33]. In the present work, we apply both energy-resolved CID studies and theory to a systematic study of the occurrence of the direct $b_2 \rightarrow a_1$ reaction.

Experimental

The experimental work was carried out using an electrospray/quadrupole/time-of-flight (QqToF) mass spectrometer (QStar XL; SCIEX, Concord, Canada). The work reported here involved quasi-MS^3 studies of fragment ions. In this approach CID in the interface region produced fragment ions with those of interest being selected by the quadrupole Q for CID in the collision cell q and analysis of the products by the time-of-flight analyzer. The cone voltage in the interface region was varied to give the best yield of the b_2 ion of interest; the CID mass spectra of the b_2 ions (MS^3) were independent of the cone voltage employed to generate the precursor b_2 ions. By varying the collision energy in the quadrupole cell q breakdown graphs, expressing the relative ion signals as a function of collision energy, were constructed.

Ionization was by electrospray with the sample, at micromolar concentration in 1:1 CH_3OH:1% aqueous formic acid, being introduced into the source at a flow rate of 10 $\mu L min^{-1}$. Nitrogen was used as nebulizing gas and drying gas and as collision gas in the quadrupole collision cell.

The peptides Ala-Sar-Ala-Ala-Tyr-Ala and Tyr-Sar-Ala-Ala-Ala-Ala were obtained from Celtek Peptides (Nashville, TN, USA). All other peptide samples were obtained from Bachem Biosciences (King of Prussia, PA, USA). None showed impurities in their mass spectra and they were used as received.

Computational Methods

Density functional theory calculations were performed with the Gaussian 09 suite of programs [36]. Multiple minima, transition structures, and product ion geometries were optimized with the B3LYP [37–39] and M06-2X [40, 41] functionals. The 6-31+G(d,p) basis set was employed and local energy minima were confirmed with frequency calculations. Multiple transition structures (TSs) for both the critical b_2–a_1 and b_2–a_2 bond cleavage reactions and those occurring within the resulting proton-bound dimers were investigated for a suite of b_2 ions with the following sequences: GlyGly, AlaGly, ValGly, TyrGly, GlySar (Sar=N-methylglycine), AlaSar, TyrSar, $GlySarF_3$ (where the N-CH_3 in Sar is replaced with N-CF_3), AlaPro, ValPro, ProPro. This enabled comparison of theory to experimental results and also extrapolation to related compounds. The results of the two computational methods were compared with our experimental findings and also to each other. A *t*-test was performed to determine if there was any statistical difference for the two methods for the two reaction types.

Experimental Results

Breakdown graphs were obtained for the b_2 ions derived from Ala-Gly-Ala, Val-Gly-Gly, Leu-Gly-Gly, Val-Ala-p-NA (Val-Ala-para-nitroanilide), Phe-Gly-Gly, Tyr-Gly-Gly, and Phe-Leu-NH_2. All these b_2 ions are expected to have a protonated oxazolone structure. For the first four cases, the only product ions observed were the a_2 ion and the a_1 ion. For the Phe-Gly and Tyr-Gly b_2 ions, in addition to the a_2 and a_1 ions, a minor signal is observed at *m/z* 132 and 148, respectively, in addition to the respective a_n ions (Figure 1). For both cases, these minor ions result from elimination of CO+NH_3 from the a_2 ion [42].

The a_2 ions readily undergo further fragmentation to form a_1 ions, as has been observed previously [34]. For the a_2 ions derived from b_2 ions where the Gly residue was part of the oxazolone ring in the original b_2 ions no signal for the Gly iminium ions were observed. Similarly, the a_2 ion derived from Val-Ala did not fragment to give the Ala iminium ion. This is logical if proton affinities (PAs) are considered as the departing C-terminal Gly/Ala imine has substantially lower PA (~205, 208, and ~215, 217 kcal/mol, values for Gly and Ala from M06-2X, B3LYP/6-31+G(d,p) levels of theory, respectively) than the larger N-terminal residue/imine. The calculated imine proton affinities are in reasonable agreement with those calculated previously [34]. On the other hand (Figure 2), both the Phe iminium ion (*m/z* 120) and the Leu iminium ion (*m/z* 86) are observed on fragmentation of the a_2 ion derived from the

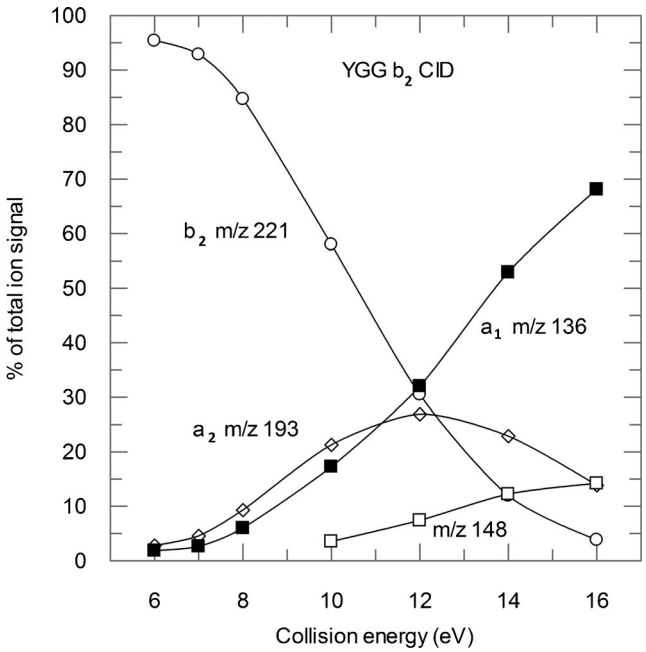

Figure 1. Breakdown graph for the Tyr-Gly b_2 ion derived from Tyr-Gly-Gly

Phe-Leu b_2 ion, indicating that the much larger leucine imine has a competitive proton affinity with the Phe imine. This is in agreement with earlier observations [34]. It is also clear from Figure 2 that in this case the b_2 ion does not fragment directly to the a_1 ion to any significant extent at low collision energies.

The ready fragmentation of a_2 ions to form the relevant a_1 ions creates some difficulties in determining the branching ratio for direct formation of a_2 and a_1 ions from b_2 ions. Table 1 records the observed a_1/a_2 ratios in fragmentation of six b_2 ions as a function of collision energy. Over the lowest collision energy range 6–8 eV, the ratios remain essentially constant but increase as the collision energy is increased further, probably because of the increasing impact of the $a_2 \rightarrow a_1$ fragmentation reaction. As Figures 1 and 2 show, the extent of fragmentation of the b_2 ion is relatively small at 6–8 eV collision energy and it appears that the a_1/a_2 ratios measured at these low collision energies may provide a reasonable estimate of the branching ratio for fragmentation of the respective b_2 ions. Support for this assertion comes from earlier metastable ion studies. Yalcin et al. [10] reported that metastable ion fragmentation of the Leu-Gly b_2 ion gave an a_1/a_2 ratio of 2.0. Ambihapathy et al. [35] reported an a_1/a_2 ratio of 0.44 in the metastable ion fragmentation of the Phe-Gly b_2 ion. A more extensive study of the metastable ion fragmentation of b_2 ions was reported by Harrison et al. [15] using fast atom bombardment ionization and B/E linked scans on an EB double-focussing mass spectrometer. They reported an a_1/a_2 ratio of 0.16 for fragmentation of the Ala-Gly b_2 ion, an a_1/a_2 ratio of 1.1 for fragmentation of the Leu-Gly b_2 ion, and an a_1/a_2 ratio of 0.55 for fragmentation of the Phe-Gly b_2 ion. They also reported an a_1/a_2 ratio of 0.10 for metastable ion fragmentation of the Val-Ala b_2 ion. For correctness, we note that the present experimental study does not provide unambiguous evidence for the exclusive formation of the a_1 ion upon direct fragmentation of the b_2 ion, fragmentation observed at lower CID energies may provide information on the relative energies on the $b_2 \rightarrow a_1$, $b_2 \rightarrow a_2$, and even the $a_2 \rightarrow a_1$ processes. Table 1 additionally illustrates an experimental trend as a function of the size of the aliphatic N-terminal residue (Ala-Gly→Val-Gly→Leu-Gly) whereby the ratio of a_1/a_2 increases with size. This is presumably due to the increased ability to stabilize the protonated imine leaving group in the $b_2 \rightarrow a_1$ transition structure and products. Evidence in support of this is provided by our density functional theory calculations (Table 2), which show a clear reduction in the $b_2 \rightarrow a_1$ barrier as the N-terminal residue increases in size [Gly→Ala→Val; 40.9→31.2→29.2 kcal/mol, M06-2X/6-31+G(d,p)]. A small concomitant but consistent rise in the $b_2 \rightarrow a_2$ barrier is also observed, which naturally complements the reduction in $b_2 \rightarrow a_1$ barrier. The Val-Gly b_2 ion breakdown graph is provided in Supplementary Figure S1.

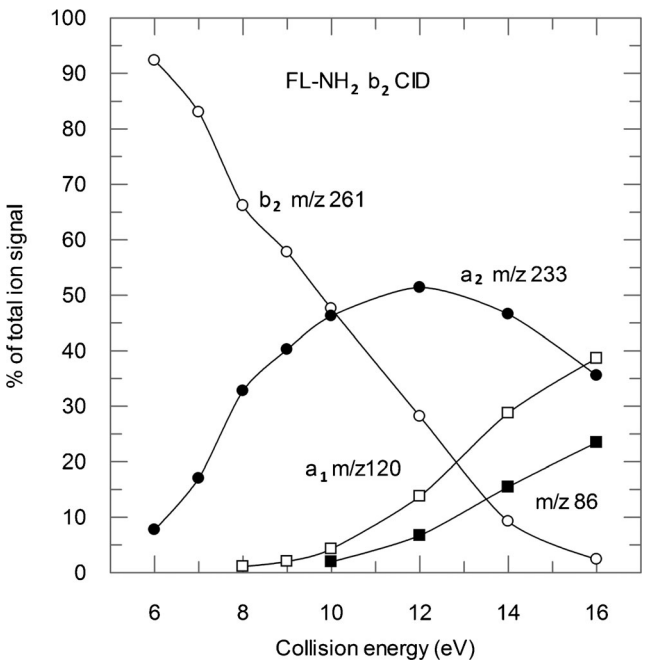

Figure 2. Breakdown graph for the Phe-Leu b_2 ion derived from Phe-Leu-NH_2

Mechanistic Considerations

The fragmentation reactions of simple oxazolone b_2 ions have been studied in detail involving threshold CID and computational studies by Siu and co-workers [32, 33] and by Armentrout and Clark [31]. These studies have established detailed pathways for the $b_2 \rightarrow a_2$ and $b_2 \rightarrow a_1$ fragmentation reactions. A simplified version of the pathway for the $b_2 \rightarrow a_2$ fragmentation is shown in Scheme 1. Initially, it was believed [10, 35, 43] that the a_2 ion was a substituted imine ion shown as

Table 1. a_1/a_2 Ratio in Fragmentation of Oxazolone b_2 Ions. The m* is for Metastable Ion Fragmentation of Ions Produced by Fast Atom Bombardment [15]

Laboratory collision energy/eV	Sequence of oxazolone b_2 ion					
	AlaGly	ValGly	LeuGly	PheGly	TyrGly	ValAla
6.0	0.38	1.7	1.8	0.55	0.66	0.0
7.0	0.39	1.6	1.9	0.52	0.57	0.13
8.0	0.44	1.7	2.0	0.54	0.64	0.18
9.0	-	1.9	2.2	-	-	0.25
10.0	0.65	2.4	2.6	0.77	0.81	0.39
12.0	1.1	3.1	3.7	1.2	1.2	0.95
14.0	2.1	5.3	6.7	2.6	2.3	2.5
16.0	4.1	10.4	13.4	5.9	4.9	6.3
m*	0.16	-	1.1	0.55	-	0.10

a_2 in Scheme 1. However, the computational studies [31–33] as well as IRMPD studies [44–46] have shown that the cyclic structure is more stable and can be readily formed (Scheme 1). It should be noted that the calculations show [31–33] that the transition state for loss of CO is considerably higher than the energies of either a_2 or a_1 products. This is in agreement with observations [10, 35] that there is considerable release of kinetic energy in the metastable ion fragmentation of b_2 ions to a_2 ions.

A somewhat simplified version of the pathway elucidated [31–33] for the $b_2 \rightarrow a_1$ fragmentation reaction is presented in Scheme 2. The essential features involve cleavage of the bond between the carbon of the oxazolone ring and the R_1CHNH_2 group. This is followed by transfer of a proton from the side-chain amine function to the carbon of the oxazolone ring and transfer back of the hydrogen attached to the nitrogen of the oxazolone ring and cleavage to give the a_1 iminium ion. The highest energy structure is TS1, which is only slightly higher in energy than the final products. This is consistent with the observation [35] that the metastable ion fragmentation reaction $b_2 \rightarrow a_1$ involves only a small release of kinetic energy.

Support for the fragmentation pathway outlined in Scheme 2 comes from our observation that when the nitrogen of the oxazolone ring does not bear a hydrogen atom, a_1 ion formation from the b_2 ion does not occur but rather the b_2 ion eliminates a neutral imine. Consequently, the $b_2 \rightarrow a_1$ pathway can either produce a protonated imine (a_1 immonium ion) if the final proton transfer occurs or if this does not occur and dimer separation occurs an N-terminally truncated protonated oxazolone is produced. Figure 3 shows the breakdown graph for the Ala-Sar b_2 ion (Sar=*N*-methylglycine). There is minor formation of the a_2 ion (*m/z* 115); however, the major primary fragmentation pathway results in formation of *m/z* 100, corresponding to elimination of $CH_3CH{=}NH$ from the b_2 ion producing an oxazolone ring with a H atom rather than the $CH_3CH\text{-}NH_2$ group on its nominally N-terminal side (i.e., bonded to the carbonyl carbon of residue 1; alanine). The *m/z* 100 product fragments further by successive elimination of CO neutrals. The energetics of this process are supported by our density functional theory calculations, which clearly show a preference for the $b_2 \rightarrow a_1$ fragmentation reaction (barrier, ΔH_{0K}=23.1, 27.6 kcal/mol, Table 2) and its *m/z* 100 products (25.1, 34.0 kcal/mol, Supplementary Table S1) relative to the $b_2 \rightarrow a_2$ pathway, which is limited by the comparatively high energy transition structure that requires at least 38.1, 37.8 kcal/mol to access (Table 2). A similar experimental result is obtained (Figure 4) for fragmentation of the Tyr-Sar b_2 ion. Again, elimination of the neutral Tyr imine (135 u) to form *m/z* 100 is the major primary fragmentation pathway. A similar result has been reported by Wysocki and co-workers [47], who observed that the b_2 ion derived from Val-(*N*-methyl-Ala)-Ala-Pro-Arg fragmented exclusively by loss of a neutral of 71 u,

Table 2. Relative Energies of the Oxazolone b_2 Ion Fragmentation Barriers Determined at the B3LYP/6-31+G(d,p) and M06-2X/6-31+G(d,p) Levels of Theory

Oxazolone, b_2 ion sequence	B3LYP/6-31+G(d,p)		M06-2X/6-31+G(d,p)	
	b_2-a_2 TS, ΔH_{0K} (ΔG_{298})/ kcal mol^{-1}	b_2-a_1TS, ΔH_{0K} (ΔG_{298})/ kcal mol^{-1}	b_2-a_2 TS, ΔH_{0K} (ΔG_{298})/ kcal mol^{-1}	b_2-a_1 TS, ΔH_{0K} (ΔG_{298})/ kcal mol^{-1}
GlyGly	32.8 (30.7)	38.5 (37.0)	33.7 (31.7)	40.9 (39.5)
AlaGly	33.7 (31.7)	27.4 (25.9)	34.5 (32.8)	31.2 (29.7)
ValGly	34.7 (32.6)	24.3 (23.0)	35.5 (33.5)	29.2 (28.0)
TyrGly	34.5 (32.7)	26.2 (24.7)	35.7 (34.4)	31.4 (30.3)
GlySar	36.7 (35.4)	34.3 (33.2)	36.3 (35.3)	36.9 (36.1)
AlaSar	38.1 (36.8)	23.1 (21.5)	37.8 (36.7)	27.6 (26.4)
TyrSar	39.1 (38.0)	21.4 (20.2)	41.8 (39.5)	29.1 (27.1)
$GlySarF_3$	34.4 (32.6)	25.7 (23.8)	35.1 (33.1)	29.3 (26.2)
AlaPro	28.7 (28.1)	26.8 (25.7)	28.5 (27.5)	31.4 (30.0)
ValPro	29.8 (29.0)	26.8 (24.5)	29.9 (29.1)	32.2 (30.5)
ProPro	29.8 (29.1)	20.7 (19.1)	30.5 (28.1)	26.9 (25.0)

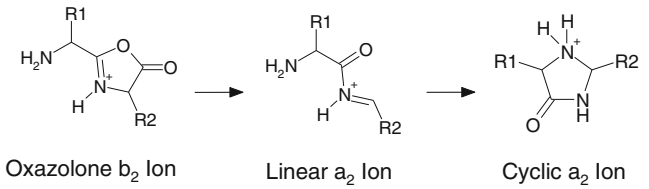

Scheme 1. A simplified $b_2 \rightarrow a_2$ fragmentation pathway

which was shown to correspond in composition to the neutral Val imine. In terms of the pathway of Scheme 2, the final H-transfer from the nitrogen of the oxazolone is blocked by the methyl group of the *N*-methyl-glycine and *N*-methyl-alanine, with the result that neutral imine elimination is observed as the dominant primary fragmentation pathway of the b_2 ion. Minor formation of the Tyr iminium ion (*m/z* 136) is observed at higher collision energies. Our calculations predict a post-carbon–carbon bond cleavage, proton-bond dimer comprised of a protonated Tyr iminium ion hydrogen-bonded to a neutral "zwitterion" Sar oxazolone ring (Figure 5). Nominally, this leaves the ring with a fixed positive charge from the N–CH_3 and a negative C as it only has three bonds to it (a carbanion). Practically, the calculations indicate that this charge is more delocalized. The neutral, "zwitterion" Sar oxazolone ring has a PA of ~230, 233 kcal/mol versus the Tyr imine, which is ~223, 225 kcal/mol depending on the computational model. Consequently, the PA of the tyrosine imine is apparently high enough to keep the proton at least some of the time, presumably when the complex has at least 6–8 kcal/mol more energy than the lowest energy form, which fits with the experimental finding of this only occurring at higher collision energy, separation prior to an equilibrium being set up in the dimer.

Computational Studies

(1) Problems with Models? Our computational findings are summarized in Table 2 and the Supporting Information (Supplementary Tables S1 and S2). This encompasses 11 rationally selected oxazolone b_2 ion systems and two model chemistries. While the trends predicted by the two models are very similar,

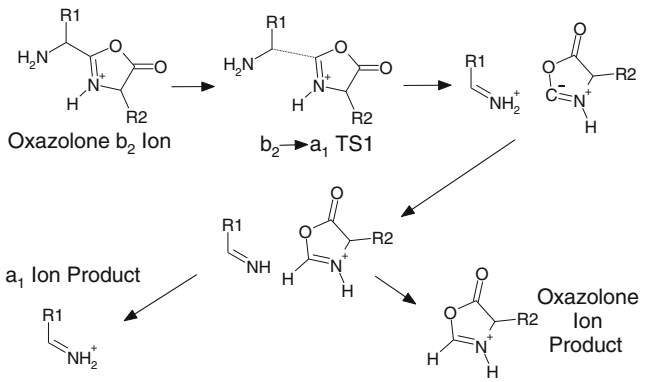

Scheme 2. A simplified version of the $b_2 \rightarrow a_1$ fragmentation pathway [31–33]

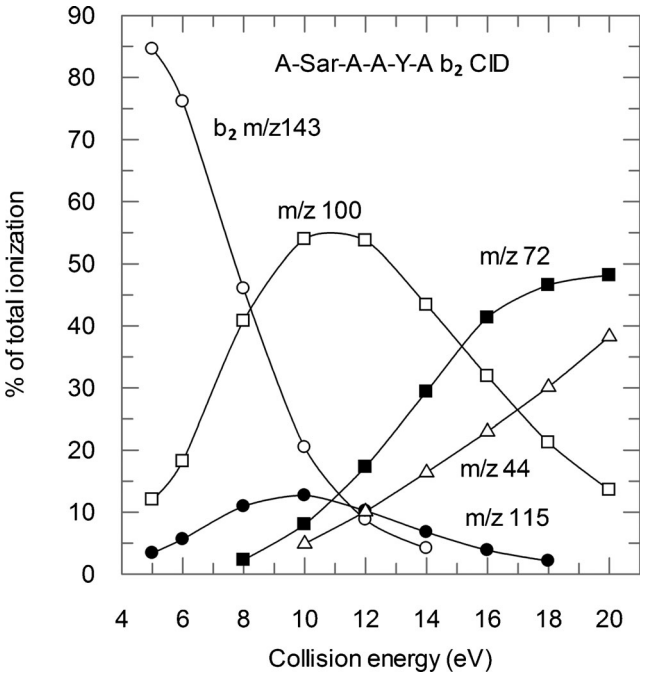

Figure 3. Breakdown graph for the Ala-Sar b_2 ion derived from Ala-Sar-Ala-Ala-Tyr-Ala

the relative energies underlying them are less consistent, particularly for the b_2-a_1 reaction. In fact, based solely on the B3LYP/6-31+G(d,p) barriers for the b_2-a_1 and b_2-a_2 reactions, you would expect the b_2-a_1 reaction to be the dominant source of product ions in all cases except GlyGly. Our experimental findings do not support this proposal. In contrast the M06-2X/6-31+G(d,p) values predict substantially higher barriers for the

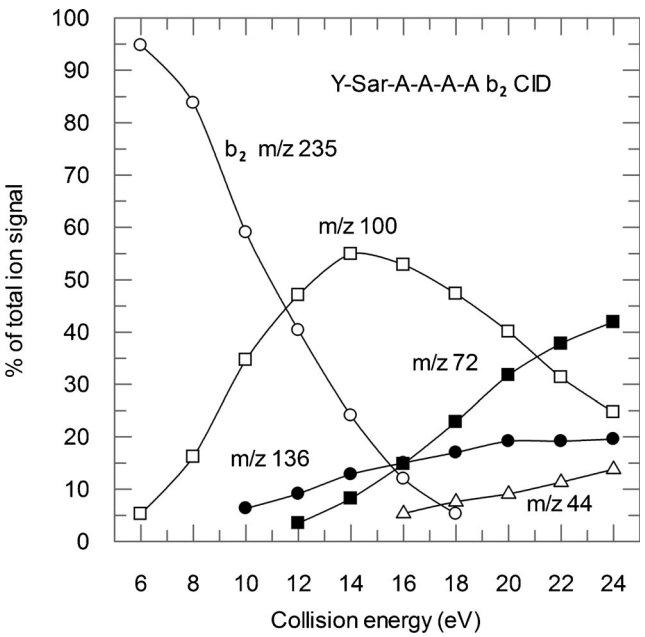

Figure 4. Breakdown graph for the Tyr-Sar b_2 ion derived from Tyr-Sar-Ala-Ala-Ala-Ala

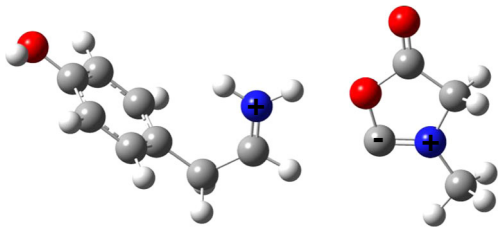

Figure 5. Tyr-Sar b_2 oxazolone fragmentation; the $b_2 \rightarrow a_1$ reaction post-carbon-carbon bond cleavage, proton-bond dimer comprised of a protonated Tyr iminium ion hydrogen-bonded to a neutral "zwitterion" Sar oxazolone ring

b_2-a_1 reactions, resulting in much more similar barriers to the b_2-a_2 pathway; the b_2-a_1 barrier is still often the more favorable pathway though. Practically, this means the presence of both types of a_n product ion is now supported by theory. To assess whether the two models really were producing statistically different values, we utilized a paired *t*-test for comparing individual differences [48] to investigate the two methods for each fragmentation reaction. For the b_2-a_2 reaction measurements, we find t_{calc}=2.301 and with $t_{table,95\%}$=2.262 (i.e., this is technically, a significant difference between the models, but it is right on the border of non-significance). For example, removal of one data point returns the result to being not significant. Consequently, without additional data, it is not clear if the effect is real or just fortuitous for the b_2-a_2 reaction measurements. In contrast, the b_2-a_1 reaction measurements provide a much stronger case for significant differences between the methods; t_{calc}=9.497, which is substantially greater than t_{table} even at 99.9% confidence ($t_{table,99.9\%}$=4.781), indicates a significant difference between the methods is present. Why does B3LYP perform so poorly (and differently) for the b_2-a_1 reaction? The b_2-a_1 reaction transition structure is structurally similar to S_N2-type reactions. The B3LYP functional has been shown to systematically underestimate the activation barrier height calculations for S_N2 reactions by "overestimating the nondynamical electron correlation" and thereby providing spurious stability to systems (i.e., lowering the energy) [49, 50]. Thus, B3LYP barriers from these types of calculations should be viewed as lower bounds/estimates for the reaction [51, 52]. The much more recent M06-2X method does not appear to suffer from these issues. In light of these findings, we shall utilize the M06-2X/6-31+G(d,p) values for the remainder of the discussion.

(2) Trends and Predictions from Theory Our calculations are in general agreement with those performed previously by the Siu and Armentrout groups [31–33] on Gly- and Ala-containing oxazolone b_2 ions. We extend the preceding analyses to additional systems to probe the effect of systematic N-terminal/C-terminal residue change (Table 2, Supplementary Tables S1 and S2). Our combined calculations and experimental work indicate that there is likely a greater prevalence of the $b_2 \rightarrow a_1$ reaction than had previously been imagined. This is probably due to the multiple means of generating a_1 ions and also experimental discrimination against low *m/z* ions in general. Additionally, we provide evidence for some trends based on our electronic structure calculations. For example, by increasing the size of the N-terminal alkyl residue, we see a reduction of the calculated $b_2 \rightarrow a_1$ barrier. This is likely due to the increased $b_2 \rightarrow a_1$ transition structure charge stabilization provided by the departing protonated imine alkyl side chain. A concomitant increase in the $b_2 \rightarrow a_2$ barrier is also observed. Furthermore, the presence of an N-terminal aryl side chain seems to have a stabilizing effect on the $b_2 \rightarrow a_1$ TS relative to the shorter alkyl chains (H, CH_3).

Going from a C-terminal Gly residue to the fixed charge Sar residue (*N*-methylglycine) results in an increase in the $b_2 \rightarrow a_2$ barrier, which is most prevalent when the N-terminal residue is larger. A corresponding decrease in the $b_2 \rightarrow a_1$ barrier is observed too. N-terminal Gly is still substantially less favorable than other, larger residues for this reaction because of its limited ability to stabilize the transition structure. Switching the C-terminal Sar residue for $SarF_3$ (*N*-trifluoromethylglycine) results in a small decrease in the b_2-a_2 barrier and in contrast to the non-fluorinated systems, the $b_2 \rightarrow a_1$ barrier is significantly reduced too (7.6 kcal/mol). The difference for the $b_2 \rightarrow a_2$ barrier is due to a change in the nature of the hydrogen bonding in the transition structure providing additional stability. The $GlySarF_3$ form has a rotated N-terminus so that H···F bonds are formed between the electronegative fluorine atoms and an N-terminal hydrogen and one of the C_{alpha} hydrogens. Why then the huge difference for the b_2-a_1 barrier? As the leaving group involved in the TS (formation of $H_2N^+{=}CH_2$) remains unchanged and the general arrangement of the atoms is very similar here, the effect is likely due to the effect of having the electron withdrawing CF_3 group adjacent to the charged ring nitrogen. This is inherently unstable as is pulls electron density away from the cation, which in turn has the effect of increasing the likelihood of the $b_2 \rightarrow a_1$ reaction, as this reaction transfers electron density toward the nitrogen to form a net neutral species.

It has been reported [53] and confirmed in this laboratory (AGH), that a major fragmentation channel of the Pro-Pro b_2 ion involves elimination of a neutral imine, possibly cyclic, to form a fragment ion of *m/z* 126. On the surface, this would seem to be analogous to the imine elimination reactions discussed above, and we have extended the computational analysis to study the fragmentation of the Ala-Pro, Val-Pro, and Pro-Pro b_2 ions with oxazolone structures (Table 2). The results of this analysis show that for the Ala-Pro and Val-Pro b_2 ions, fragmentation to form a_2 ions is slightly favored over imine elimination. This is consistent with the experimental observation (unpublished results) that these b_2 ions fragment primarily to form a_2 ions with only minor elimination of an imine to form *m/z* 126. On the other hand, the calculations indicate that for the oxazolone form of the Pro-Pro, b_2 ion fragmentation by imine elimination is favored substantially over CO elimination to form the a_2 ion. However, there are complications. Although it has been shown [29] that the Ala-

Pro and Val-Pro b_2 ions are formed primarily with an oxazolone structure, very recent work by Oomens and co-workers [54] has led to the conclusion that the Pro-Pro b_2 ion has a protonated diketopiperazine structure rather than an oxazolone structure when generated from small polyprolines. As yet, it is unclear whether the Pro-Pro b_2 ion is always a diketopiperazine structure irrespective of precursor ion sequence (or charge state). For the purposes of the present discussion of energetics, we will proceed from the premise that a b_2 oxazolone structure might be formable under the correct circumstances.

Our computational analysis of oxazolone b_2 ions containing C-terminal Proline (Pro) residues illustrates a modest increase in the $b_2 \rightarrow a_2$ barrier as the N-terminal residue increases in size. Despite the increased size of the N-terminal residue in the ValPro b_2 ion, we see essentially no change (and perhaps a slight increase) in the $b_2 \rightarrow a_1$ barrier relative to the AlaPro congener. This is due to the bulk of the Val side chain limiting the favorable hydrogen bonding possibilities in the transition structure. Consequently, the benefit of having a much more stabilized leaving group is confounded by the inability to hydrogen bond as effectively with the adjacent oxazolone ring oxygen. Lastly, the ProPro oxazolone $b_2 \rightarrow a_1$ reaction involves a less bulky, secondary imine leaving group, which has a larger proton affinity [~221 kcal/mol, M06-2X/6-31+G(d,p)] than either the Val (~219 kcal/mol) or Ala (~215 kcal/mol) congeners. Consequently, it is not surprising that this $b_2 \rightarrow a_1$ reaction has the lowest energy barrier of the systems calculated here.

Conclusions

Experimentally, the present study shows that oxazolone b_2 ions with the Gly residue as part of the oxazolone ring fragment not only by CO elimination to form the a_2 ion but also, in part, fragment directly to form the a_1 ion. Indeed, in a number of systems the a_1 ion is more abundant than the a_2 ion near the threshold for fragmentation. The computational studies of the transition state energies for the $b_2 \rightarrow a_2$ channel and the $b_2 \rightarrow a_1$ channel show that, with the exception of the Gly-Gly b_2 ion, the transition state energies are similar, making formation of a_1 competitive with formation of a_2.When the nitrogen of the oxazolone ring does not bear a hydrogen, as in the Ala-Sar and Tyr-Sar b_2 ions, the final proton transfer step leading to a_1 formation (Scheme 2) cannot take place and a neutral imine is eliminated instead. Again the computational studies show that this is the most favorable fragmentation pathway.

Finally, significant differences ($P<0.001$) between the M06-2X and B3LYP models were found when investigating the $b_2 \rightarrow a_1$. Based on the experimental findings, B3LYP systematically underestimates these barriers, whereas the M06-2X model appears to be much more realistic. The computations provide further evidence of the limitations of the B3LYP functional when describing S_N2-like reactions.

Acknowledgment

The authors acknowledge support for this work by start-up funds from the University of Missouri-St. Louis and a University of Missouri-St. Louis College of Arts and Sciences Research Grant. Calculations were performed locally and at the University of Missouri Bioinformatics Consortium (UMBC).

References

1. Paizs, B., Suhai, S.: Fragmentation pathways of protonated peptides. Mass Spectrom. Rev. **24**, 508–548 (2005)
2. Roepstorff, P., Fohlman, J.: Proposals for a common nomenclature for sequence ions in mass spectra of peptides. Biomed. Mass Spectrom. **11**, 601 (1984)
3. Biemann, K.: Contributions of mass spectrometry to peptide and protein structure. Biomed. Environ. Mass Spectrom. **16**, 99–111 (1988)
4. Mueller, D.R., Eckersley, M., Richter, W.: Hydrogen transfer reactions in the formation of "Y+2" sequence ions from protonated peptides. Org. Mass Spectrom. **23**, 217–222 (1988)
5. Cordero, M.M., Houser, J.J., Wesdemiotis, C.: The neutral products formed during backbone cleavage of protonated peptides in tandem mass spectrometry. Anal. Chem. **65**, 1594–1601 (1993)
6. Tsang, C.W., Harrison, A.G.: The chemical ionization of amino acids. J. Am. Chem. Soc. **98**, 1301–1308 (1976)
7. Van Dongen, W.D., Heerma, W., Haverkamp, J., de Koster, C.G.: The B_1 fragment from protonated glycine is electrostatically-bound ion/molecule of $CH_2{=}NH_2^+$and CO. Rapid Commun. Mass Spectrom. **10**, 1237–1239 (1996)
8. Rodriquez, C.F., Vukovic, A.H., Milburn, R.K., Hopkinson, A.C.: Destabilized carbocations. A comparison of C_2H_4NS and C_2H_4NO potential energy surface. J. Molec. Struct. (Theochem.) **404**, 112–125 (1997)
9. Bythell, B.J., Csonka, I.P., Suhai, S., Barofsky, D.F., Paizs, B.: Gas-phase structure and fragmentation pathways of singly-protonated peptides with N-terminal arginine. J. Phys. Chem. B **114**, 15092–15105 (2010)
10. Yalcin, T., Khouw, C., Csizmadia, I.G., Peterson, M.R., Harrison, A.G.: Why are B ions stable species in peptide mass spectra? J. Am. Soc. Mass Spectrom. **6**, 1165–1174 (1995)
11. Yalcin, T., Csizmadia, I.G., Peterson, M.R., Harrison, A.G.: The structures and fragmentation of B_n ($n \geq 3$) ions in peptide mass spectra. J. Am. Soc. Mass Spectrom. **7**, 233–242 (1996)
12. Nold, M.J., Wesdemiotis, C., Yalcin, T., Harrison, A.G.: Amide bond dissociation in protonated peptides. Structures of the N-terminal ionic and neutral fragments. Int. J. Mass Spectrom. Ion Process. **164**, 137–153 (1997)
13. Paizs, B., Lendvay, G., Vékey, K., Suhai, S.: Formation of b_2^+ ions from protonated peptides. Rapid Commun. Mass Spectrom. **17**, 523–533 (1999)
14. Reid, G.E., Simpson, R.J., O'Hair, R.A.J.: Probing the fragmentation reactions of protonated glycine oligomers via multistage mass spectrometry and gas phase ion molecule hydrogen/deuterium exchange. Int. J. Mass Spectrom. **190/191**, 209–230 (1999)
15. Harrison, A.G., Csizmadia, I.G., Tang, T.-H.: Structure and fragmentation of b_2 ions in peptide mass spectra. J. Am. Soc. Mass Spectrom. **11**, 427–436 (2000)
16. Rodriquez, C.F., Shoeib, T., Chu, I.K., Siu, K.W.M., Hopkinson, A.C.: Comparison between protonation, lithiation, and argentination of 5-oxazolones. A study of a key intermediate in gas-phase peptide sequencing. J. Phys. Chem. A **104**, 5335–5342 (2000)
17. Somogyi, Á.: Probing peptide fragment ion structures by combining sustained off-resonance collision-induced dissociation and gas-phase H/D exchange (SORI-HDX) in Fourier transform ion-cyclotron resonance (FT-ICR). J. Am. Soc. Mass Spectrom. **19**, 1771–1775 (2008)
18. Bythell, B.J., Somogyi, Á., Paizs, B.: What is the structure of b_2 ions generated from doubly protonated tryptic peptides? J. Am. Soc. Mass Spectrom. **20**, 618–624 (2009)
19. Harrison, A.G.: To b or not to b. The ongoing saga of peptide b ions. Mass Spectrom. Rev. **28**, 640–654 (2009)
20. Bythell, B.J., Hendrickson, C.L., Marshall, A.G.: Relative stability of peptide sequence ions generated by tandem mass spectrometry. J. Am. Soc. Mass Spectrom. **23**, 644–654 (2012)
21. Polfer, N.C., Oomens, J., Suhai, S., Paizs, B.: Spectroscopic and theoretical evidence for oxazolone ring formation in collision-induced dissociation of peptides. J. Am. Chem. Soc. **127**, 17154–17155 (2005)

22. Polfer, N.C., Oomens, J., Suhai, S., Paizs, B.: Infrared spectroscopy and theoretical studies on gas-phase Leu-enkephalin and its fragments. Direct experimental evidence for the mobile proton. J. Am. Chem. Soc. **129**, 5887–5897 (2007)
23. Yoon, S.-H., Chamot-Rooke, J., Perkins, B.R., Hilderbrand, A.E., Poutsma, J.C., Wysocki, V.H.: IRMPD spectroscopy shows that AGG forms an oxazolone b_2^+ ion. J. Am. Chem. Soc. **130**, 17644–17645 (2008)
24. Oomens, J., Young, S., Molesworth, S., Van Stipdonk, M.: Spectroscopic evidence for an oxazolone structure of the b_2 fragment from protonated trialanine. J. Am. Soc. Mass Spectrom. **20**, 334–339 (2009)
25. Bythell, B.J., Erlekam, U., Paizs, B., Ma tre, P.: Infrared spectroscopy of fragments derived from tryptic peptides. Chem. Phys. Chem. **10**, 883–885 (2009)
26. Farrugia, J.M., Taverner, T., O'Hair, R.A.J.: Side chain involvement in the fragmentation reactions of the protonated methyl esters of histidine and its peptides. Int. J. Mass Spectrom. **209**, 99–112 (2001)
27. Perkins, B.R., Chamot-Rooke, J., Yoon, S.H., Gucinski, A.C., Somogyi, Á., Wysocki, V.H.: Evidence of diketopiperazine and oxazolone structures for HA b_2^+ion. J. Am. Chem. Soc. **131**, 17528–17529 (2009)
28. Gucinski, A.C., Chamot-Rooke, J., Nicol, E., Somogyi, Á., Wysocki, V.H.: Structural influences on preferential oxazolone versus diketopiperazine b_2^+ ion formation for histidine analogue-containing peptides. J. Phys. Chem. A **116**, 4296–4304 (2012)
29. Gucinski, A.C., Chamot-Rooke, J., Steinmetz, V., Somogyi, Á., Wysocki, V.H.: Influence of N-terminal residue composition on the structure of proline-containing b_2^+ ions. J. Phys. Chem. A **117**, 1291–1298 (2013)
30. Zou, S., Oomens, J., Polfer, N.C.: Competition between diketopiperazine and oxazolone formation in water loss products from Arg-Gly and Gly-Arg. Int. J. Mass Spectrom. **316/318**, 12–17 (2012)
31. Armentrout, P.B., Clark, A.A.: The simplest b_2^+ ion: determining its structure from its energetics by a direct comparison of the threshold collision-induced dissociation of protonated oxazolone and diketopiperazine. Int. J. Mass Spectrom. **316/318**, 182–191 (2012)
32. El Aribi, H., Rodriquez, C.F., Almeida, D.R.P., Ling, M., Mak, W.W.-N., Hopkinson, A.C., Siu, K.W.M.: Elucidation of fragmentation mechanisms of protonated peptide ions and their products. A case study on glycylglycylglycine using density functional theory and threshold collision-induced dissociation. J. Am. Chem. Soc. **125**, 9229–9236 (2003)
33. El Aribi, H., Orlova, G., Rodriquez, C.F., Almeida, D.R.P., Hopkinson, A.C., Siu, K.W.M.: Fragmentation mechanisms of product ions from protonated tripeptides. J. Phys. Chem. B **108**, 18743–18749 (2004)
34. Harrison, A.G., Young, A.B.., Schnoelzer, M., Paizs, B.: Formation of iminium ions by fragmentation of a_2 ions. Rapid Commun. Mass Spectrom. **18**, 1635–1640 (2004)
35. Ambihapathy, K., Yalcin, T., Leung, H.-W., Harrison, A.G.: Pathways to immonium ions in the fragmentation of protonated peptides. J. Mass Spectrom. **32**, 209–215 (1997)
36. Frisch, M.J. , Trucks, G.W., Schlegel, H.B., Scuseria, G.E., Robb, M.A., Cheeseman, J.R., Scalmani, G., Barone, V., Mennucci, B., Petersson, G.A., Nakatsuji, H., Caricato, M., Li, X., Hratchian, H.P., Izmaylov, A.F., Bloino, J., Zheng, G., Sonnenberg, J.L., Hada, M., Ehara, M., Toyota, K., Fukuda, R., Hasegawa, J., Ishida, M., Nakajima, T., Honda, Y., Kitao, O., Nakai, H., Vreven, T., Montgomery, J.A., Peralta, J.E., Ogliaro, F., Bearpark, M., Heyd, J.J., Brothers, E., Kudin, K.N., Staroverov, V.N., Keith, T., Kobayashi, R., Normand, J., Raghavachari, K., Rendell, A., Burant, J.C., Iyengar, S.S., Tomasi, J., Cossi, M., Rega, N., Millam, J.M., Klene, M., Knox, J.E., Cross, J.B., Bakken, V., Adamo, C., Jaramillo, J., Gomperts, R., Stratmann, R.E., Yazyev, O., Austin, A.J., Cammi, R., Pomelli, C., Ochterski, J.W., Martin, R.L., Morokuma, K., Zakrzewski, V.G., Voth, G.A., Salvador, P., Dannenberg, J.J., Dapprich, S., Daniels, A.D., Farkas, O., Foresman, J.B., Ortiz, J.V., Cioslowski, J., Fox, D.J.: *Gaussian 09, Revision C.01*; Gaussian, Inc.: Wallingford CT (2010)
37. Becke, A.D.: Correlation energy of an inhomogeneous electron gas: a coordinate-space. J. Chem. Phys. **88**, 1053–1062 (1988)
38. Stephens, P.J., Devlin, J.F., Chabalowski, C.F., Frisch, M.J.: Ab initio calculation of vibrational absorption and circular dichroism spectra using density functional force fields. J. Phys. Chem. **98**, 11623–11627 (1994)
39. Lee, C., Yang, W., Parr, R.G.: Development of the Colle-Salvetti correlation energy formula into a functional of the electron density. Phys. Rev. B **37**, 785–789 (1988)
40. Zhao, Y., Schultz, N.E., Truhlar, D.G.: Exchange-correlation functional with broad accuracy for metallic and non-metallic compounds, kinetics, and noncovalent interactions. J. Chem. Phys. **123**(16)), 161103 (2005)
41. Zhao, Y., Truhlar, D.G.: The M06 suite of density functionals for main group thermochemistry, thermochemical kinetics, noncovalent interactions, excited states, and transition elements: two new functionals and systematic testing of four M06-class functionals and 12 other functionals. Theor. Chem. Acc. **120**, 215 (2006)
42. Bythell, B.J., Hernandez, O., Steinmetz, V., Paizs, B., Maître, P.: Tyrosine side-chain catalyzed proton transfer in the YG a_2 ion revealed by theory and IR spectroscopy in the "fingerprint" and X—H (X=C, N, O) stretching region. Int. J. Mass Spectrom. **316/318**, 227–234 (2012)
43. Paizs, B., Szlávik, Z., Lendvay, G., Vékey, K., Suhai, S.: Formation of a_2^+ ions of protonated peptides. An ab initio study. Rapid Commun. Mass Spectrom. **14**, 746–755 (2000)
44. Bythell, B.J., Ma tre, P., Paizs, B.: Cyclization and rearrangement reactions of a_n fragment ions of protonated peptides. J. Am. Chem. Soc. **132**, 14766–14779 (2010)
45. Verkerk, U.H., Siu, C.-K., Steill, J.D., El Aribi, H., Zhao, J., Rodriquez, C.F., Oomens, J., Hopkinson, A.C., Siu, K.W.M.: a_2 ion derived from triglycine: an N_1-protonated 4-imidazolidinone. J. Phys. Chem. Lett. **1**, 868–872 (2010)
46. Verkerk, U.H., Zhao, J., Lau, J.K.-C., Lam, T.-W., Hao, Q., Steill, J.D., Siu, C.-K., Oomens, J., Hopkinson, A.C., Siu, K.W.M.: Structures of the a_2 ions of Ala-Ala-Ala and Phe-Phe-Phe. Int. J. Mass Spectrom. **330/332**, 254–261 (2012)
47. Smith, L.L., Hermann, K.A., Wysocki, V.H.: Investigation of gas-phase ion structures for proline-containing b_2 ions. J. Am. Soc. Mass Spectrom. **17**, 20–28 (2006)
48. Harris, D.C.: Quantitative Chemical Analysis, 8th ed. W.H. Freeman and Company: New York, pp. 78–79 (2010)
49. Gritsenko, O.V., Ensing, B., Schipper, P.R.T., Baerends, E.J.: Comparison of the accurate Kohn-Sham solution with the generalized gradient approximations (GGAs) for the S_N2 Reaction F-+CH_3F ->FCH_3+F-: a qualitative rule to predict success or failure of GGAs. J. Phys. Chem. A **104**, 8558–8565 (2000)
50. Laerdahl, J.K., Uggerud, E.: Gas phase nucleophilic substitution. Int. J. Mass Spectrom. **214**, 277–314 (2002)
51. Bythell, B.J., Barofsky, D.F., Pingitore, F., Polce, M.J., Wang, P., Wesdemiotis, C., Paizs, B.: Backbone cleavages and sequential loss of carbon monoxide and ammonia from protonated AGG: a combined tandem mass spectrometry, isotope labeling, and theoretical study. J. Am. Soc. Mass Spectrom. **18**, 1291–1303 (2007)
52. Bleiholder, C., Paizs, B.: Competing gas-phase fragmentation pathways of asparagine-, glutamine-, and lysine-containing protonated dipeptides. Theor. Chem. Acc. **125**, 387–396 (2010)
53. Grewal, R.N., El Aribi, H., Harrison, A.G., Siu, K.W.M., Hopkinson, A.C.: Fragmentation of protonated tripeptides: the proline effect revisited. J. Phys. Chem. B **108**, 4899–4908 (2004)
54. Martens, J.K., Grzetic, J., Berden, G., Oomens, J.: Gas-phase conformations of small polyprolines and their fragment ions by IRMPD spectroscopy. Int. J. Mass Spectrom. (2014). doi:10.1016/j.ijms.2014.07.027